PROTEINS: Structure, Function, and Genetics 36:270–281 (1999)

# RESEARCH ARTICLES

## Macromolecular Impurities and Disorder in Protein Crystals

**C.L. Caylor,[1] I. Dobrianov,[1] S.G. Lemay,[1] C. Kimmer,[1] S. Kriminski,[1] K.D. Finkelstein,[2] W. Zipfel,[3] W.W. Webb,[3] B.R. Thomas,[4] A.A. Chernov,[4] and R.E. Thorne[1]***

[1]*Laboratory of Atomic and Solid State Physics, Cornell University, Ithaca, New York*
[2]*Cornell High-Energy Synchrotron Source (CHESS), Ithaca, New York*
[3]*Department of Applied and Engineering Physics, Cornell University, Ithaca, New York*
[4]*Center for Microgravity and Materials Research, University of Alabama in Huntsville, Huntsville, Alabama*

***ABSTRACT*** **The mechanisms by which macromolecular impurities degrade the diffraction properties of protein crystals have been investigated using X-ray topography, high-resolution diffraction line shape measurements, crystallographic data collection, chemical analysis, and two-photon excitation fluorescence microscopy. Hen egg-white lysozyme crystals grown from solutions containing a structurally unrelated protein (ovotransferrin) and a related protein (turkey egg-white lysozyme) can exhibit significantly broadened mosaicity due to formation of cracks and dislocations but have overall B factors and diffraction resolutions comparable to those of crystals grown from uncontaminated lysozyme. Direct fluorescence imaging of the three-dimensional impurity distribution shows that impurities incorporate with different densities in sectors formed by growth on different crystal faces, and that impurity densities in the crystal core and along boundaries between growth sectors can be much larger than in other parts of the crystal. These nonuniformities create stresses that drive formation of the defects responsible for the mosaic broadening. Our results provide a rationale for the use of seeding to obtain high-quality crystals from heavily contaminated solutions and have implications for the use of crystallization for protein purification. Proteins 1999;36:270–281.** © 1999 Wiley-Liss, Inc.

**Key words: crystal growth; crystal defects; protein crystallography; X-ray topography; fluorescence microscopy**

### INTRODUCTION

High-resolution X-ray structures of biological macromolecules required for the most complete understanding of biological processes can only be obtained using high-quality macromolecular crystals. One of the most important factors affecting crystal and diffraction quality is growth solution purity.[1–3] Growth solutions can contain a wide variety of macromolecular impurities including structurally-related genetic variants, variants produced by post-translational modifications such as deglycosylation, deamidation, partial denaturation, and dimerization, as well as structurally unrelated molecules. Total solution impurity concentrations are typically at least several molecular percent, and even high-purity commercial lysozymes have impurity concentrations of at least one percent.[4–8] These impurities can have profound effects on crystal growth, producing reduced or increased solubility, suppressed or enhanced nucleation, and changes in growth habit and morphology, and are often responsible for the irreproducibility of crystallization experiments.[4–16] Impurities can significantly degrade crystal quality, causing dislocations and cracks, formation of twins and polycrystalline and amorphous aggregates, and degradation of crystal mosaicity and diffraction resolution.[5,8,9,14,17,18]

Most fundamental studies of impurity effects in macromolecular crystallization have focused on lysozyme. Light scattering studies show that impurities can broaden the distribution of molecular aggregate sizes in undersaturated solutions (most likely due to heterogeneous association of lysozyme with the impurities) and that this polydispersity correlates with the formation of ill-shaped and twinned crystals.[5,6] Analyses of crystals using electrophoresis, chromatography, and mass spectrometry indicate that structurally-related impurities (e.g., related avian lysozymes) are incorporated in substantial concentrations, whereas structurally unrelated impurities (e.g., ovalbumin, ribonuclease A) are usually rejected by the growing crystal.[5,6,9,12–14,16,18] Optical microscopy and interferometry studies indicate that impurities inhibit growth step motion, reduce growth rates, and lead to macrostep formation.[13,16] Atomic force microscopy studies have directly

Grant sponsor: NASA; Grant numbers: NAG8-1357, NAG8-1574, NAG8-1454, and NCC8-66CC; Grant sponsor: USRA; Grant sponsor: National Science Foundation; Grant number: BIR/CB1-9419978; Grant sponsor: Department of Education Fellowship; Grant sponsor: National Institutes of Health; Grant number: P412RR04224.

*Correspondence to: R.E. Thorne, Physics Department, Clark Hall, Cornell University, Ithaca, NY 14853. E-mail: ret6@cornell.edu

Received 7 January 1999; Accepted 19 April 1999

observed growth step pinning by adsorbed macromolecular impurities and have established that this pinning is responsible for cessation of growth.[19,20] Added impurities in solution make more visible the growth bands produced when crystal growth rates change abruptly, suggesting that impurity incorporation depends on growth rate.[8,17] This growth-rate dependence has recently been confirmed by fluorescence microscopy imaging of incorporated fluorescently-labeled impurities.[21]

Despite this progress, a number of basic issues remain unresolved. These include: (1) How are impurities distributed within a crystal? (2) How do impurities create disorder, and what kinds of disorder are created? and (3) How do the various kinds of disorder affect the diffraction properties of interest to crystallographers?

We have investigated the effects of macromolecular impurities on the quality of lysozyme crystals using a combination of X-ray topography, high-resolution lineshape measurements, standard oscillation X-ray data collection, chemical analysis, and two-photon excitation fluorescence microscopy. The impurities studied have little effect on crystal B factors and diffraction resolutions but create cracks and dislocations that strongly affect mosaicity. This disorder appears to arise from nonuniform impurity incorporation and can in some cases be largely eliminated using a simple seeding technique. Our results have implications both for crystal growth and for the use of crystallization for purification.

## MATERIALS AND METHODS

Tetragonal hen egg-white lysozyme (HEWL) crystals were grown by the batch method in 10 μl hanging drops. Growth solutions contained high-purity commercial HEWL (Seikagaku, 6 times recrystallized) at concentrations between 20 and 30 mg/ml dissolved in 0.1 M acetate buffer at pH 4.5, and ~0.75 M NaCl. Two different impurities were investigated: ovotransferrin and turkey egg-white lysozyme (TEWL), both from Sigma. Ovotransferrin (MW = 78 kDa) is a structurally unrelated protein sometimes found as an impurity in commercial lysozyme. TEWL (MW = 14.5 kDa) differs from HEWL (MW = 14.6 kDa) in only seven of its 129 residues. This homologous protein thus serves as a simple model for a heterogeneous form of HEWL.

X-ray measurements were performed at the Cornell High-Energy Synchrotron Source (CHESS) on stations B-2 and C-2, using Si (111) double bounce monochromators to select an incident X-ray wavelength of 1.24 Å. X-ray topography measurements were performed by illuminating the crystal with an unfocused, highly parallel incident beam and recording the resulting diffraction pattern using high-resolution film (Kodak Industrex SR) placed ~3 cm from the crystal. Under these conditions, the Bragg spots provide two-dimensional images of the crystal, and image contrast arises due to variations in lattice orientation and spacing from point to point in the crystal.[22] Topography allows imaging of protein crystal mosaicity and strain arising from defects such as dislocations, cracks, twins, inclusions, and grain boundaries, as well as from sectoriality and crystal bending.[23–31] For the incident beam parameters and sample-to-film distance used, the spatial resolution of the images is a few microns under optimum conditions and the sensitivity to lattice orientation variations is roughly 0.003°.

High-resolution measurements of diffraction peak line shapes were performed using a six-circle Huber diffractometer, a Si (111) analyzer crystal, and a Bicron scintillation detector. Mosaic (ω) scans were performed by rocking the crystal about an axis perpendicular to the scattering plane and recording the diffracted intensity in a given peak at fixed detector angle 2θ.[32–34] θ–2θ scans were performed by rocking the detector by twice the rocking angle of the crystal. These two types of scan provide information about the distribution of lattice plane orientations and spacings, respectively, within the crystal.[27] To maximize instrumental resolution, most measurements were performed near $2\theta \approx 23°$, the Bragg angle for Si (111). The corresponding resolutions for mosaic and θ–2θ scans are $\Delta\theta \approx 0.003°$ and $\Delta(2\theta) \approx 0.003°$, respectively.

Oscillation diffraction patterns were recorded using image plates. Partial data sets were analyzed using Scalepak and DENZO to determine lattice parameters, and subroutines from the CCP4 package were used to perform a Wilson analysis to estimate overall crystal B factors and the diffraction resolution.

Incorporated concentrations of ovotransferrin and TEWL were characterized by dissolving contaminated crystals in buffer solution and analyzing the resulting solutions using SDS-PAGE with enhanced silver staining and HPLC, respectively.

Crystals for fluorescence microscopy were grown in sitting drops by the batch method from solutions containing fluorescently-labeled impurities. Impurity proteins were labeled using the Alexa 488 Protein Labeling Kit obtained from Molecular Probes. The incorporated label has MW = 520 Da, much smaller than that of the impurity molecules, although multiple labels may attach to a single impurity. Attached labels may modify incorporation behavior so that labeled molecules are best considered as distinct impurities from their unlabeled form. Two-photon excitation fluorescence microscopy measurements were performed using the facilities of the Developmental Resource for Biophysical Imaging and Electronics at Cornell. In this technique, a femtosecond infrared laser beam focused through the objective lens of a microscope excites fluorescence by a two-photon absorption process.[35,36] The amount of two-photon excitation is proportional to the intensity squared (rather than to the intensity as in one-photon excitation), so that there is very little absorption outside the focal plane and the excitation volume at the focus is well-defined both laterally and vertically. By rastering the laser across the sample and collecting the non-descanned epifluorescence using a photomultiplier, a digital image of the fluorophore distribution within a two-dimensional slab of the crystal is produced, and successive slabs are imaged by stepping the objective focus vertically. Thus, this technique allows quantitative three-dimensional mapping of the impurity distribution within the crystal. For the

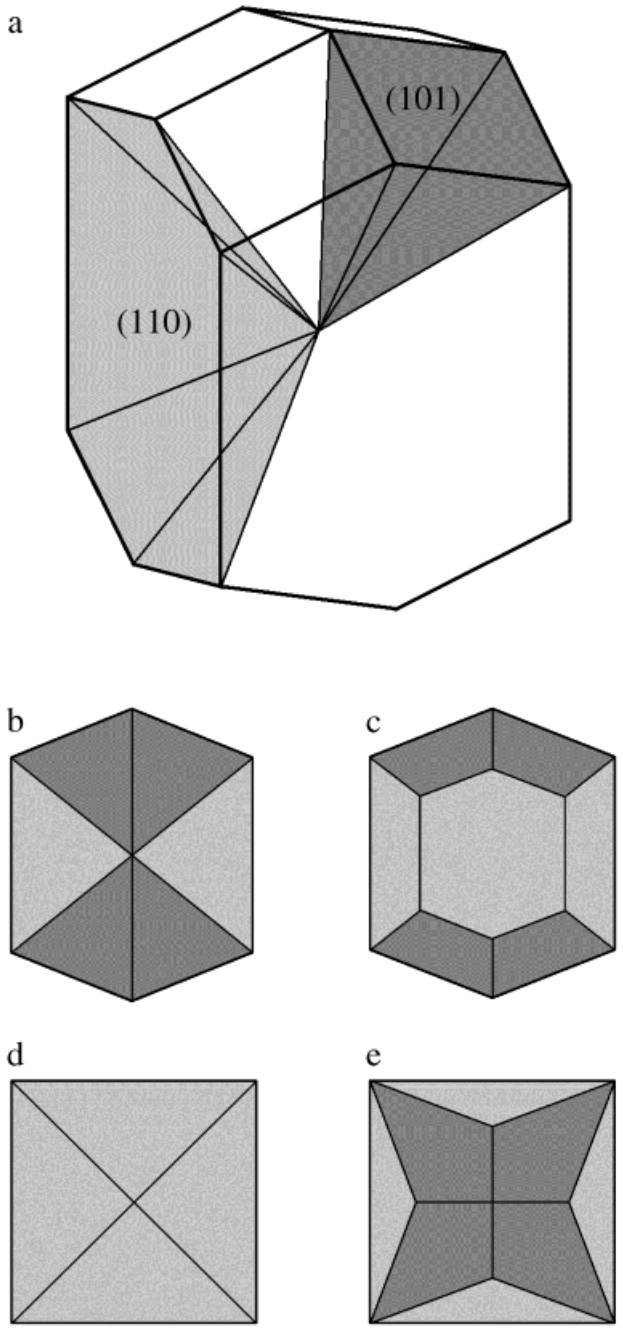


Fig. 1. **(a)** Growth habit of tetragonal hen egg-white lysozyme crystals.[17] The dark gray region is one of eight equivalent (101) sectors, and the light gray region is one of four equivalent (110) sectors. **(b-c)** Growth sector structure in thin slices parallel to a (110) face, taken through the crystal center (b) and away from the center (c). **(d-e)** Sector structure in slices perpendicular to the four-fold c-axis.

objective lens used in these experiments (10×, 0.4 NA), the lateral and axial resolutions (limited by the excitation volume and pixel size) are 1.8 μm and 10 μm, respectively.

Figure 1(a) shows the typical growth habit of a tetragonal HEWL crystal, which is formed by a combination of prismatic (110) and pyramidal (101) faces.[17] Different parts of the molecule are exposed on each type of face, so that each provides a different set of contacts to an impinging molecule.[37,38] The shaded regions in Figure 1 indicate the two inequivalent types of growth sectors, formed by addition of molecules to these two types of faces. Figure 1(b)–(e) shows the sector structure in thin slices parallel and perpendicular to the (110) faces, corresponding to possible imaging planes in two-photon fluorescence microscopy. X-ray topography also produces two-dimensional images, but these are formed by a projection of the scattering from the entire crystal volume so that sector structure is well defined in the projection only if the sector boundaries are parallel to the scattering direction.

## RESULTS

### Morphology

Ovotransferrin and TEWL both have significant effects on HEWL crystal morphology. As shown in Figure 2, ovotransferrin concentrations of ~2–5% w/w lead after several days growth to macrostep formation, and concentrations of 10% w/w and above lead to leaf-like or spherical polycrystals. Ovotransferrin concentrations above 2% cause extensive crystal cracking, although well-faceted uncracked single crystals are occasionally obtained at concentrations of <10%. TEWL causes a concentration-dependent lengthening of the crystal c axis.[9,14,15] Unlike ovotransferrin, only large TEWL concentrations (≥20%) appear to cause appreciable crystal cracking, and solution concentrations up to 50% often yield well-faceted crystals with surfaces free of macrosteps.

### X-Ray Topography

Figure 3 shows X-ray topographs of crystals grown from solutions containing 5% ovotransferrin and 10% TEWL. While crystals grown from uncontaminated solutions invariably have featureless topographs,[27] those grown from ovotransferrin-containing solutions tend to show extensive contrast indicating the presence of cracks and dislocations. Crystals grown from TEWL solutions usually show less dramatic contrast. Some crystals (e.g., Fig. 3(a),(c),(d)) show differences in diffracted intensity from different growth sectors, indicating a difference in orientation, lattice constant, or mosaicity between sectors. When crystals are oriented to maximize their visibility, growth sector boundaries are also observed (Fig. 3(d)), indicating that these boundaries have a larger mosaicity or strain distribution and are more disordered than the rest of the crystal.

### Diffraction Line Shape Measurements

Figure 4(a) compares mosaic scans for a pure HEWL crystal, a crystal grown from a 5% ovotransferrin solution, and a crystal grown from a 20% TEWL solution. Resolution-corrected mosaic full widths at half maximum (FWHM) for 2–5% ovotransferrin and 5–20% TEWL crystals are typically 0.01 to 0.03°, much broader than those for crystals grown from uncontaminated solutions (~0.002 to 0.006°),[27] and their line shapes tend to have a complex, multi-peak structure with very broad tails. These features are consis-

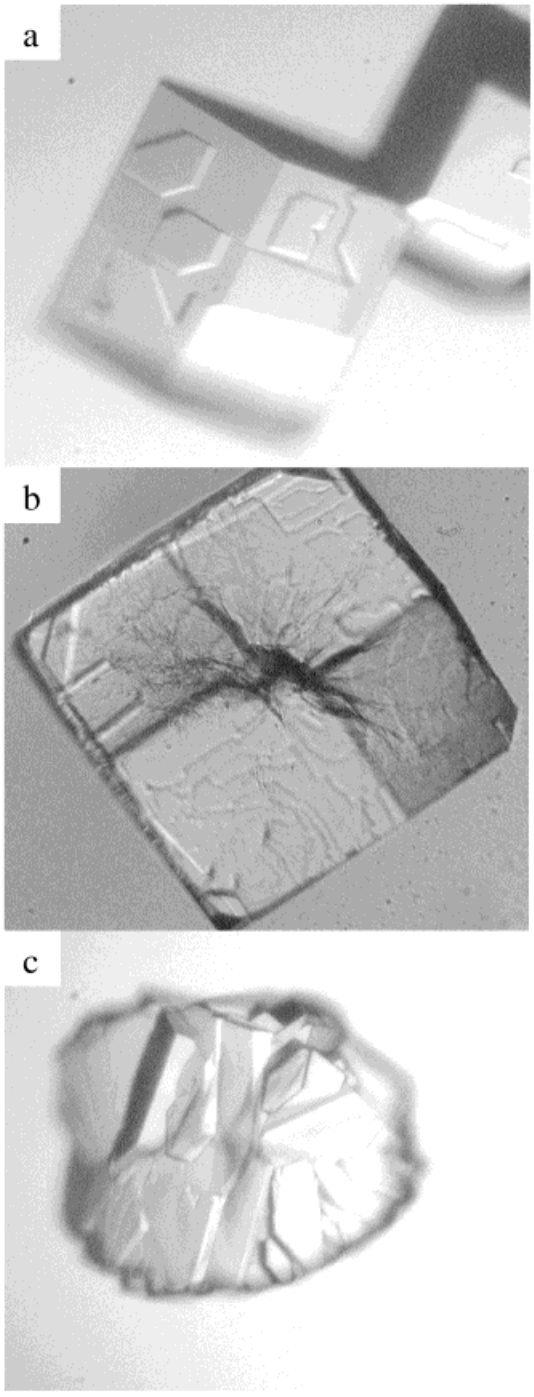


Fig. 2. Optical micrographs of tetragonal HEWL crystals grown in the presence of **(a)** 2% w/w ovotransferrin, **(b)** 5% w/w ovotransferrin, and **(c)** 10% w/w ovotransferrin. The image widths are 500 μm.

tent with the cracking and dislocations observed in the topographs.

Figure 4(b) shows corresponding θ–2θ scans. The peak widths of both the pure HEWL crystal and the 5% ovotransferrin crystal are essentially resolution limited. The peak width of the 20% TEWL crystal is significantly broadened, implying that the lattice spacing within this crystal varies. The observed resolution-corrected width is roughly 0.005°, corresponding to a fractional lattice constant variation of ~0.02%. Bulk impurity incorporation affects lattice constants because impurities occupy a different volume than the molecules they displace. Previous studies on inorganic crystals show that uniform incorporation shifts the θ–2θ peak position, and that peak broadening only occurs when incorporation is nonuniform. The results in Figure 4(b) thus indicate that TEWL is incorporated nonuniformly, and that ovotransferrin either incorporates uniformly or does not appreciably incorporate in the bulk.

### Crystallographic Diffraction Measurements

Partial crystallographic data sets were collected on more than twenty crystals, and Table I compares calculated lattice constants, B-factors, and diffraction resolutions. For crystals grown from both ovotransferrin- and TEWL-contaminated solutions, all of these parameters are identical within experimental uncertainties to those for pure HEWL crystals. Since ovotransferrin is much larger than HEWL, the absence of a lattice constant shift indicates that ovotransferrin is not appreciably incorporated in the bulk, consistent with the θ–2θ scan results. The significance of the results for TEWL is less clear because the molecular sizes of TEWL and HEWL are so similar. Assuming that the molecular volume difference is proportional to the molecular weight difference, a 20% incorporated TEWL concentration would increase the lattice constants by only 0.04%, below the ~0.06% uncertainty in the experimental values. Hirschler et al.[18] studied TEWL crystals grown from HEWL-contaminated solutions. Although chemical analysis showed incorporated HEWL concentrations of up to ~30% (corresponding to roughly 80% of its fractional concentration in solution), no effects on lattice constants or diffraction resolution were observed.

### Chemical Analysis

SDS-PAGE analysis of crystals grown from solutions containing 5% w/w ovotransferrin show no detectable amount of ovotransferrin, to a detection threshold of 0.003 % w/w. This is consistent with the absence of broadening in θ–2θ scans and implies that the segregation coefficient is less than $10^{-3}$. HPLC analysis of crystals grown from 20% w/w TEWL solutions show an incorporated TEWL concentration of ~10% w/w, implying a segregation coefficient of ~0.5, roughly consistent with the results of Hirschler et al.[18]

### Fluorescence Microscopy

Figure 5 shows representative two-photon fluorescence microscopy images of the impurity distributions in crystals grown from solutions containing 0.5% w/w fluorescently-labeled ovotransferrin. These images show several interesting features:

- The fluorescence intensity is much greater than background throughout the crystals, indicating that labeled

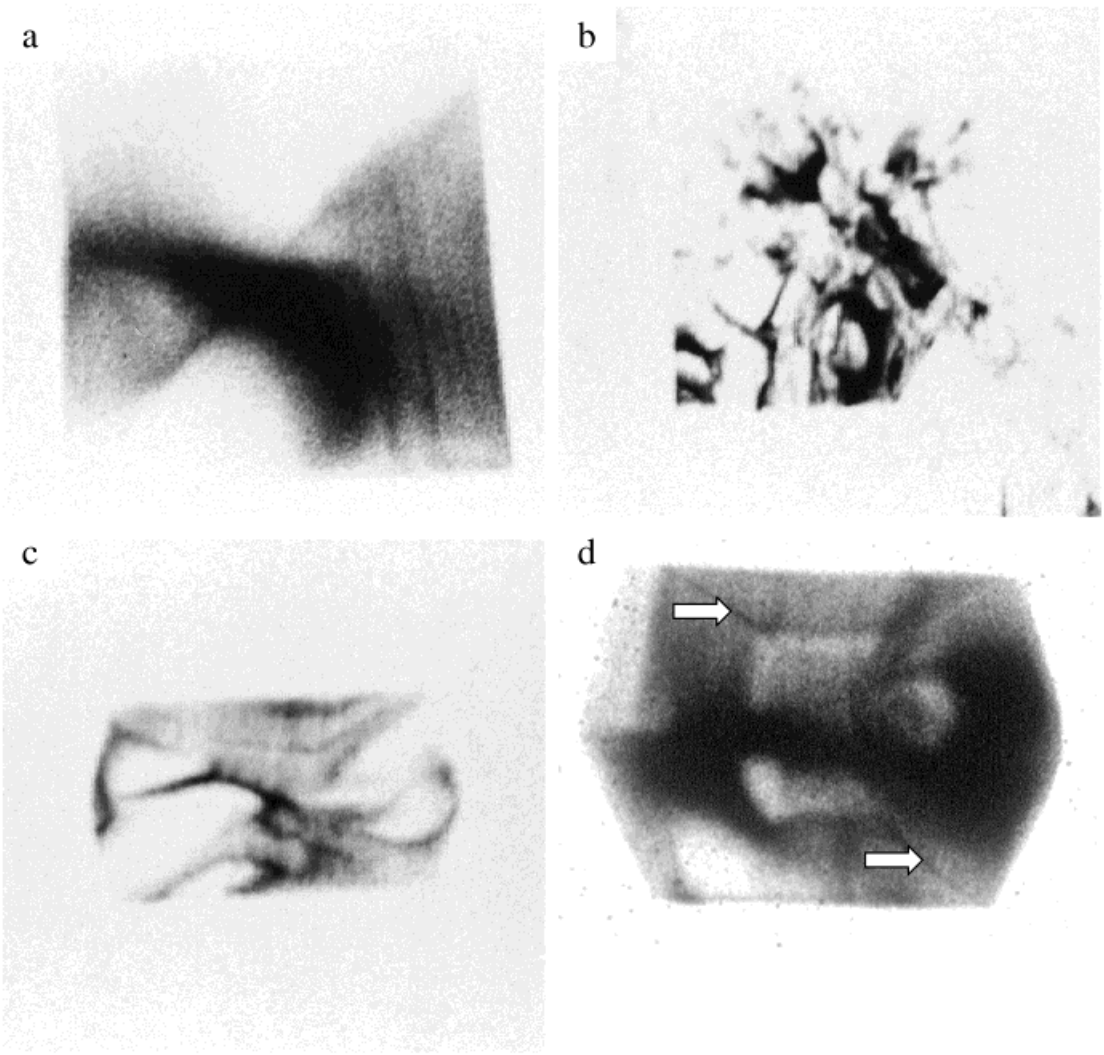


Fig. 3. X-ray topographs of HEWL crystals grown from solutions containing **(a,b)** 5% ovotransferrin and **(c,d)** 20% TEWL. The image widths are (a)–(c) 700 µm, (d) 615 µm. Arrows in (d) indicate growth sector boundaries.

ovotransferrin incorporates in the bulk. Absorbance measurements indicate that each ovotransferrin molecule has 3–4 attached labels, and fluorescence intensity calibration using a solution containing a known amount of labeled ovotransferrin yields an average incorporated density of 0.2% w/w. The corresponding segregation coefficient is ~0.4.

- The intensity differs systematically between the (110) and (101) growth sectors. Measurements on several crystals indicate an intensity ratio I(110)/I(101)~0.5–0.8.
- The boundaries between growth sectors are brighter than nearby regions, especially boundaries between inequivalent sectors which are brighter by as much as a factor of 1.5. Consequently, labeled ovotransferrin preferentially incorporate at sector boundaries, consistent with the lattice constant mismatch and higher density of lattice defects and inclusions expected there.[17,37,38]
- Visibly cracked crystals (e.g., Fig. 5(b)) have much larger impurity densities in their cores than in later growth regions. This is illustrated more clearly in Figure 6, which shows a series of images taken at various depths z in a cracked crystal, with z = 0 corresponding to the approximate location of the core. Figure 7 shows a fluorescence image, an intensity contour plot, and a plot of the intensity along a line passing through the core of another cracked crystal, where the intensity scale has been adjusted so that the core is not saturated. The core intensity is at least a factor of seven larger than that in the outer regions of the crystal, and the core diameter is roughly 50 µm. Vekilov et al.[39] found that average incorporated salt and impurity concentrations in lysozyme crystals grown from low-purity commercial lysozyme and from avidin-contaminated solutions decreased with increasing average crystal size. Based on analysis of salt incorporation

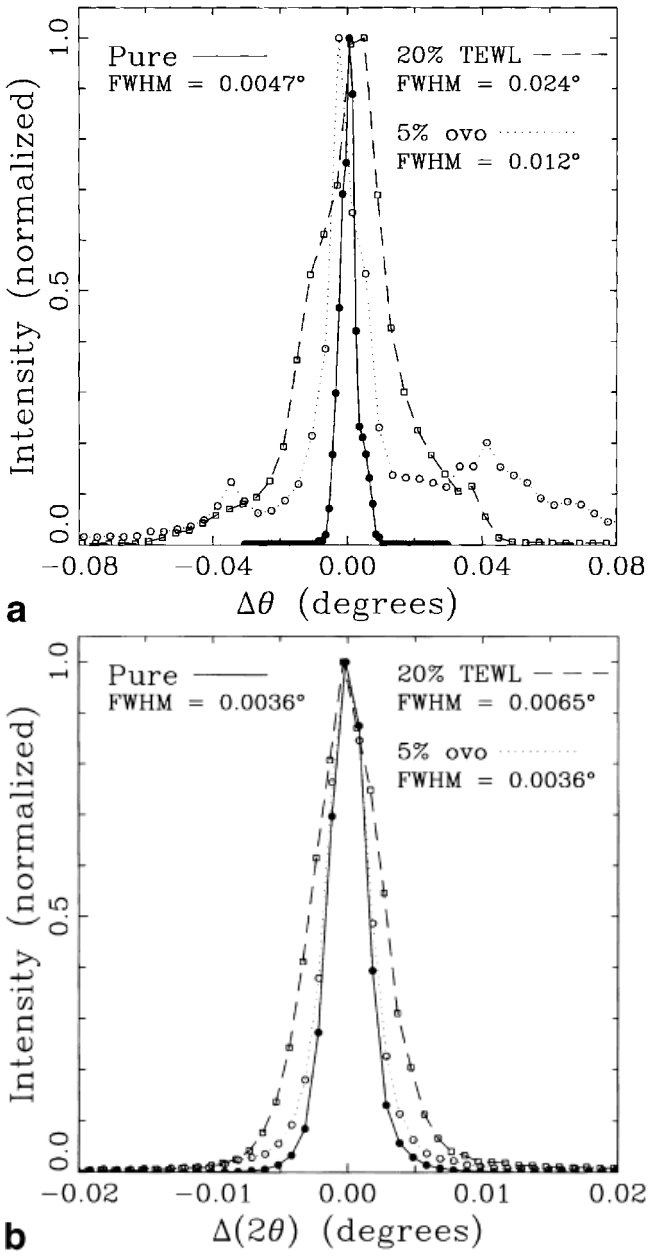


Fig. 4. **(a)** Mosaic and **(b)** θ–2θ; scans for HEWL crystals grown from an uncontaminated solution and from solutions containing 5% ovotransferrin and 20% TEWL.

and the correlation between salt and impurities, they concluded that lysozyme crystals have salt and impurity-rich cores roughly 40 μm in diameter. The data of Figures 5–7 provide direct evidence for impurity-rich cores.

- Many crystals grown from equally contaminated solutions do not crack, (e.g., Fig. 5(a)), and these crystals do not show large impurity-rich cores. Some modest enrichment does occur, however, because impurities decorate the growth sector boundaries, and the ratio of growth sector surface area to volume is largest in the core.

**TABLE I. Lattice Parameters, B Factors, and Diffraction Resolutions for Tetragonal HEWL Crystals Grown from Solutions Containing Ovotransferrin, TEWL, and Labeled Ovotransferrin**

| Crystal type | Number of crystals | a (Å) | c (Å) | B (Å²) | Resolution @ I/σ = 2 |
|---|---|---|---|---|---|
| Ovotransferrin, 2% | 2 | 79.18 | 37.99 | 18.2 | 1.57 |
| Ovotransferrin, 5% | 3 | 79.21 | 38.03 | 18.3 | 1.51 |
| Ovotransferrin, 10% | 2 | 79.21 | 38.00 | 18.6 | 1.53 |
| TEWL, 10% | 2 | 79.17 | 38.00 | 18.1 | 1.49 |
| TEWL, 20% | 4 | 79.18 | 37.93 | 17.7 | 1.55 |
| Labeled ovotransferrin, 0.5% | 2 | 79.35 | 38.06 | 17.9 | 1.53 |

Unlike unlabeled ovotransferrin, labeled ovotransferrin incorporates significantly in the crystal bulk. Because of this difference, topographs and oscillation data were collected on several crystals grown from labeled solutions. The topographs closely resemble those of unlabeled crystals and as shown in Table I, the B factors and diffraction resolutions are indistinguishable. However, the lattice parameters for labeled crystals are systematically larger: a and c are ~0.2% larger and the unit cell volume is ~0.5% larger. Assuming that the molecular volume scales with molecular weight, the observed unit cell dilation suggests an incorporated ovotransferrin concentration of ~0.4% w/w, consistent within experimental uncertainties with the concentration deduced from fluorescence measurements.

Figure 8(a) shows a fluorescence image of a crystal grown from a solution containing 0.1% w/w labeled TEWL. Like labeled ovotransferrin, labeled TEWL incorporates in the crystal bulk, with different concentrations in different growth sectors. Absorbance measurements and fluorescence intensity calibrations indicate that each TEWL molecule has on average one attached label, and incorporates with a segregation coefficient of ~0.3–0.4. Unlike labeled ovotransferrin, labeled TEWL incorporates preferentially in the (110) sectors, with I(110)/I(101)~1.3–1.4; it does not incorporate preferentially along growth sector boundaries; and it does not produce cracking or impurity-rich cores. Figure 8(b) shows a fluorescence image of a crystal grown from 0.1% w/w labeled HEWL. The image is qualitatively similar to that for labeled TEWL and yields similar sectorial concentration differences. This suggests that the incorporation behavior of both labeled TEWL and labeled HEWL may be determined by the label. Nevertheless, both labeled variants still function as well as unlabeled TEWL as models of impurities that are structurally similar to HEWL, so that our conclusions regarding such impurities should remain valid.

## DISCUSSION

### Mechanisms for Impurity Effects on Crystal and Diffraction Quality

Impurities can create crystal disorder in several ways.[37,38,40,41] First, impurities may incorporate uniformly throughout the bulk of the crystal, substituting for the host molecule or occupying sites between molecules. Local molecu-

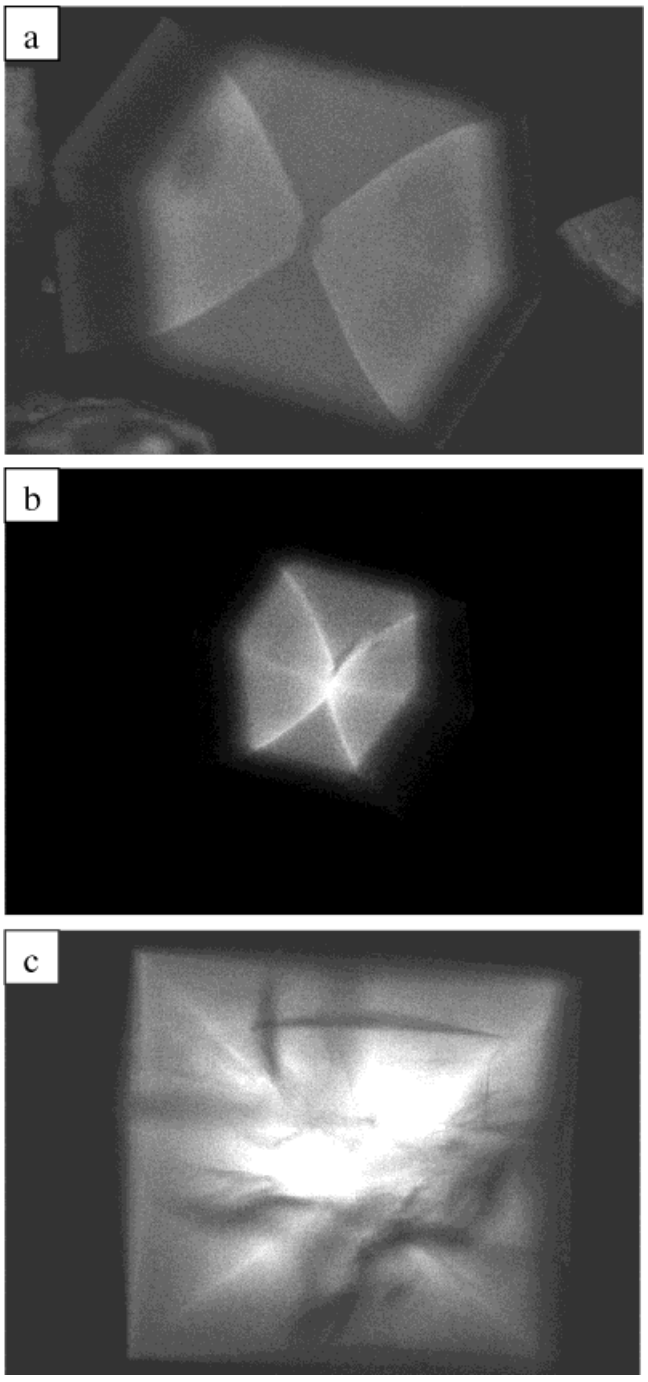


Fig. 5. Two-photon fluorescence micrographs of HEWL crystals grown from solutions containing ~0.5% labeled ovotransferrin, showing ~10 μm slices passing through the core of the crystal. The crystals in **(a)** and **(b)** are crack-free, and the crystal in **(c)** is visibly cracked. The growth solution was replaced with a fluorophore-free solution prior to data collection, so that all observed fluorescence is due to incorporated impurities. The "shadowing" on the left side of the crystal in (a) is due to reflection of light from angled crystal facets above the imaging plane. The image widths are 700 μm.

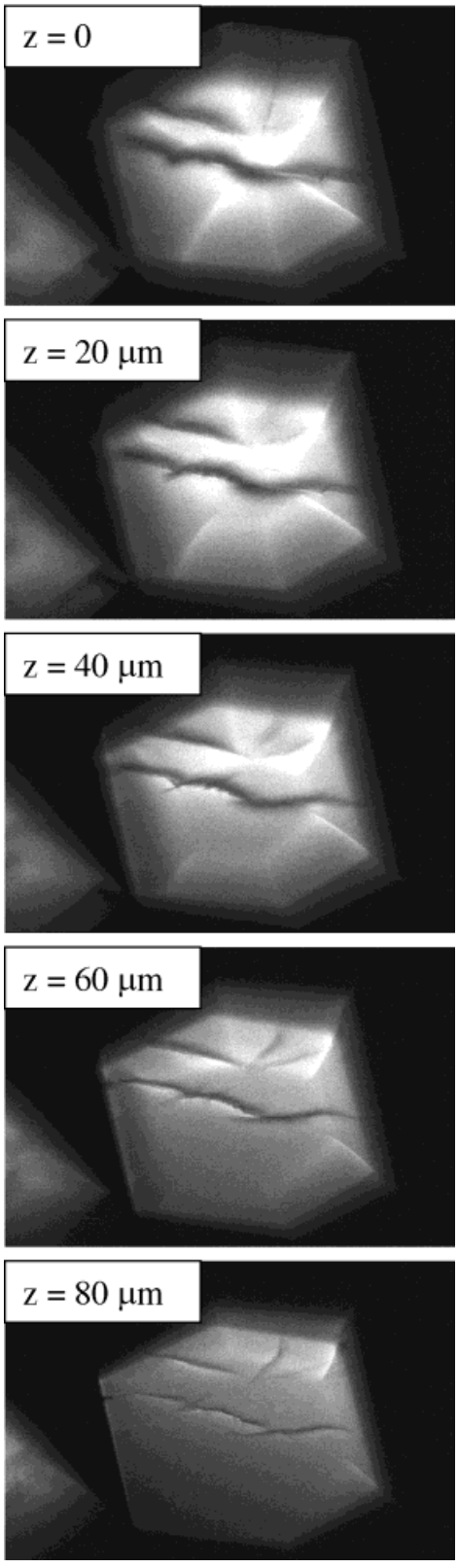


Fig. 6. Two-photon fluorescence micrographs of a HEWL crystal grown from a solution containing ~0.5% labeled ovotransferrin, acquired at successive heights z. The crystal core corresponds to z = 0. The image widths are 700 μm.

lar displacements, rotations, and conformation variations in the immediate vicinity of the impurity may affect crystal B factors (which measure short-range order), but lattice mosaicity and θ–2θ peak widths should be unaffected.

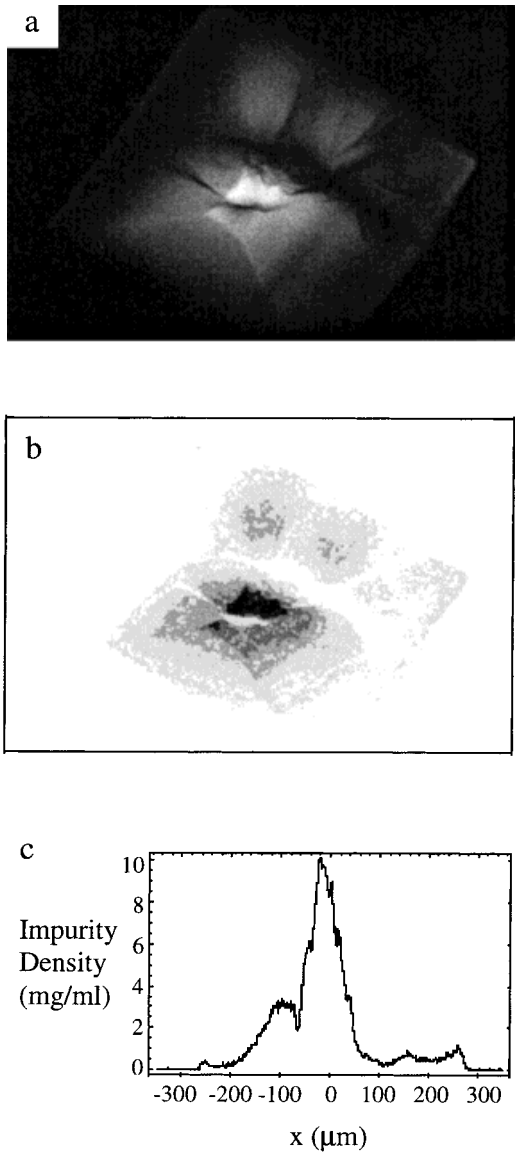


Fig. 7. **(a)** Two-photon fluorescence micrograph of a HEWL crystal grown from a solution containing ~5% labeled ovotransferrin. **(b)** A contour plot of the same data. Shades from white to black correspond to impurity concentrations of 0–1, 1–3, 3–5, 5–7, and >7 mg/cm$^3$. **(c)** Impurity concentration versus position for a narrow stripe passing through the center of the crystal in (a). The image widths in (a) and (b) are 700 μm.

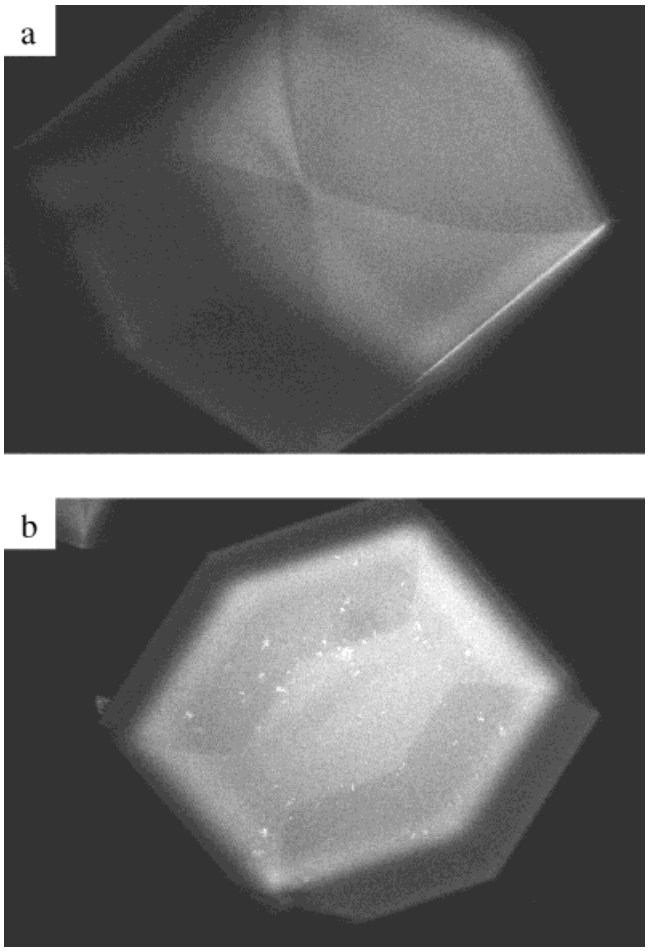


Fig. 8. Two-photon fluorescence micrographs of HEWL crystals grown from solutions containing **(a)** ~0.1% labeled TEWL and **(b)** ~0.1% labeled HEWL. The curvature of the growth sector boundaries in (a) and in Figure 5 (a) and (b) results because relative face growth rates vary with supersaturation and crystal size.[17,45] The "shadowing" of the left third of the crystal in (a) is due to reflection of light from crystal facets above the imaging plane. The image widths are 1,400 μm.

Second, impurities may incorporate with different densities in inequivalent growth sectors. Different parts of the host molecule are exposed on inequivalent crystal faces, so that impurity adsorption, surface diffusion, and incorporation rates differ. Consequently, lattice constants differ slightly between growth sectors,[37,42–44] and stresses along sector boundaries can then drive formation of dislocations and cracks.[43]

Third, impurities may incorporate nonuniformly within a given growth sector. Evolution of concentration and convective flow profiles due to protein depletion and solute rejection by the crystal cause the growth rate to decrease with time.[16,45] Since impurity incorporation depends upon growth rate,[21,38] this can produce radial variations in incorporated impurity density. For example, at high growth rates, adsorbed impurities with equilibrium segregation coefficients $<1$ can become buried by advancing growth layers before they have time to desorb. In a simple model,[37] the incorporated impurity density $n_i$ increases with the normal growth rate V and the adsorbed density $n_a$ as $n_i \propto n_a \exp(-V_c/V)$, where $V_c = H/\tau$, H is the impurity diameter, and $\tau$ is the residence time of an adsorbed impurity on an interstep terrace. Observations and simple theoretical estimates indicate that the growth rate decreases most sharply in the early stages of growth, so that this process may produce small impurity-rich cores tens of microns in diameter. These impurity density gradients produce lattice constant variations and stresses that drive defect formation. Both sectorial and radial impurity density variations should affect crystal mosaicity, but have little effect on crystal B factors in well-faceted crystals. Nonuniform impurity incorporation can also result from dynamical effects associated with step bunching but these nonuni-

formities are likely much smaller than those produced by other mechanisms.[46]

Fourth, impurities may affect ordering in the initial stages of growth. Light scattering studies indicate that protein impurities can cause formation of large aggregates in undersaturated solutions.[5,6] Aggregates containing impurities may form highly imperfect nuclei exhibiting dislocations and grain boundaries that propagate outward into subsequent growth regions. These defects will broaden crystal mosaicity but have little effect on B factors and diffraction resolutions, since away from the core the impurity density is low and the lattice should have good short-range order.

Our results for unlabeled ovotransferrin, including the absence of detectable impurity using SDS-PAGE, the absence of any lattice constant changes relative to pure crystals, and the absence of any broadening in $\theta$–$2\theta$ scans all indicate that this impurity does not incorporate appreciably in the crystal bulk, consistent with previous results for other structurally unrelated impurities including ovalbumin and ribonuclease A.[5,6,18] Consequently, ovotransferrin affects crystal quality either by incorporating significantly in the crystal core or by affecting ordering in the initial crystal nucleus.

The results for unlabeled TEWL, including its effects on crystal habit and the broadening of $\theta$–$2\theta$ scans, suggest that it does incorporate substantially in the crystal bulk (consistent with chemical analysis) but that it does so nonuniformly. This does not produce significant lattice constant changes or crystal cracking because TEWL and HEWL are so similar: the rms deviation of their $\alpha$-carbon chains is 0.46 Å, only slightly greater than the 0.37 Å deviation between HEWL in its different crystal forms.

Fluorescently-labeled TEWL exhibits directly the behavior inferred for unlabeled TEWL: it incorporates in the bulk, with different concentrations in different growth sectors (although the importance of the label in producing this behavior is unclear.) Cracking and mosaic broadening observed at larger concentrations thus likely result from stresses associated with sectorial lattice mismatches.

Unlike native ovotransferrin, fluorescently-labeled ovotransferrin incorporates appreciably in the bulk, and like labeled TEWL it shows sectorial concentration differences although with opposite sector preference. Unlike both native and labeled TEWL but like native ovotransferrin, labeled ovotransferrin produces significant cracking and other defects even at relatively low solution concentrations. Unlike labeled TEWL, labeled ovotransferrin often incorporates in much larger concentrations in crystal cores than in the bulk. This radial variation is much larger than the sector-to-sector variation, and correlates very strongly with crystal cracking. These differences and similarities suggest that the enhanced core concentration and cracking are characteristic of ovotransferrin rather than the label and that observed defects are primarily associated with the stresses produced by the radial concentration gradient.

The origin of the enhanced core impurity concentrations produced by labeled ovotransferrin is unclear. Curvature of growth sector boundaries in, e.g., Figure 5(a) indicates that face growth rates vary during growth, and this could cause impurity density variations. Using the data of Durbin and Feher,[45] the curvature in Figure 5(a) suggests that the average growth rate decreased by roughly a factor of five as the crystal grew from ~20 μm to its final size.† However, Kurihara et al.[21] found that changes in growth rate by factors of 3–7 changed the incorporated density of fluorescently-labeled avidin impurities in HEWL crystals by only 20–50%, considerably less than the factor-of-7 enhancement observed, e.g., in Figure 7. Furthermore, the impurity density is not uniform for crystal layers formed at comparable times, but instead varies with direction within a given growth sector. Another possibility is that the core may have a very high density of dislocations and other defects due to nucleation on a disordered aggregate; as at sector boundaries these defects may be decorated by impurities. This mechanism could account for the variation of impurity density with direction, and for the absence of impurity-rich cores in uncracked crystals grown from similarly contaminated solutions. However, the defect densities required to account for the large core impurity density enhancement are very large, so that some combination of these two mechanisms may be responsible for the observed impurity density variations.

Neither of the impurities or their labeled variants has any significant effect on crystal B factors or diffraction resolution. This is not surprising for native ovotransferrin (which does not incorporate in the bulk) or for TEWL (which is nearly identical in size and structure to HEWL.) However, labeled ovotransferrin has five times the molecular weight of lysozyme, and for the solution concentration studied appears to incorporate at a density of roughly 1 molecule for every 2,500 lysozyme molecules. In inorganic crystals, impurity densities of several percent cause B factor increases of only ~0.1 Å$^2$.[47] A scaling analysis suggests that macromolecular impurity densities of at least several molecular percent should be required to produce measurable effects on the much larger B factors of protein crystals.[27] This is consistent with the present results, and reflects the facts that the B factor and diffraction resolution are dominated by short range order and that impurities tend to disrupt the ordering only of their nearest neighbors.[41]

### Seeding and Impurity Effects

For impurities like ovotransferrin that cause cracking and other disorder primarily through their effects on the crystal core, one might expect to be able to grow high quality crystals from heavily contaminated solutions by providing a well-ordered seed. To test this idea, seed crystals were grown from pure commercial lysozyme, and then transferred using a Pt wire loop to solutions containing 20% ovotransferrin. Spontaneous nucleation in such heavily contaminated solutions occurs rarely, and results only in leaf- or ball-like polycrystals. As shown in Figure

†The cited result is for crystals grown from nominally pure lysozyme. Since impurities can alter growth rates, the cited growth rates may differ from those occurring in our crystals. However, since the primary effect of impurities on growth rates is at low supersaturations, our high-supersaturation growth is likely not very different from that of pure lysozome.

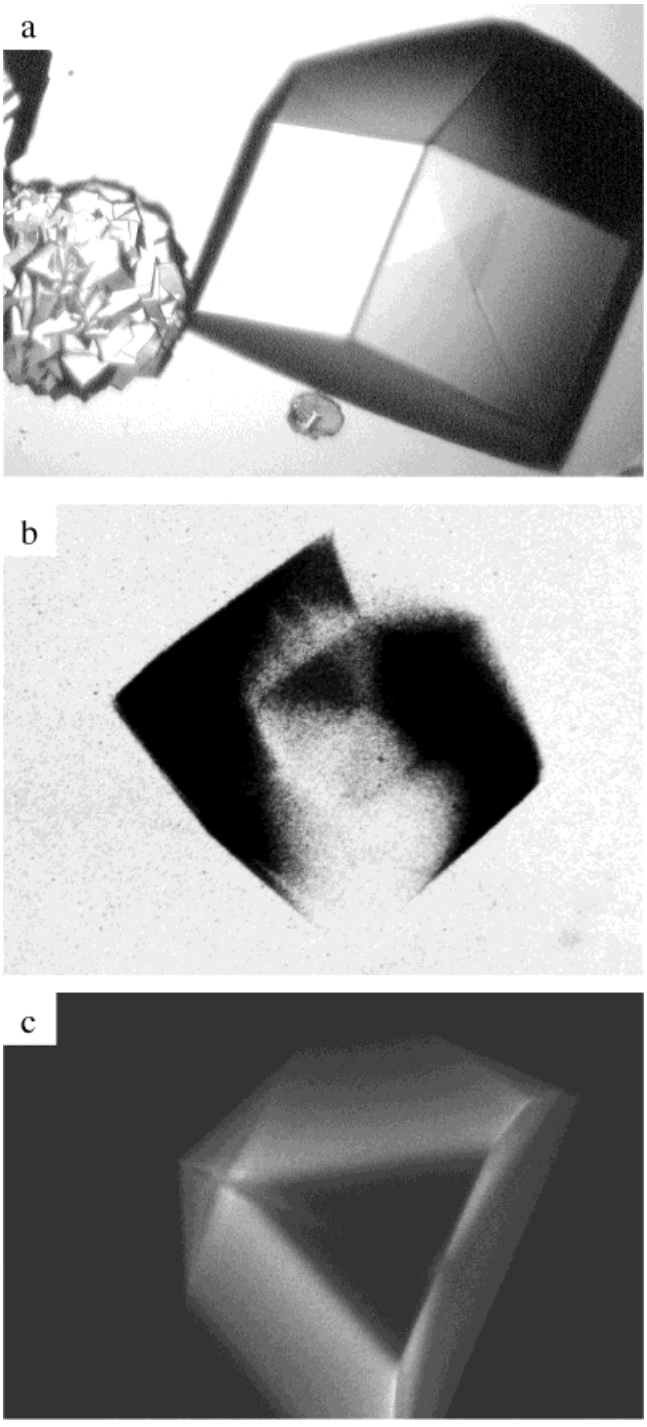


Fig. 9. **(a)** Optical micrograph of a HEWL crystal grown by transferring a pure seed to a solution containing 20% ovotransferrin. A polycrystalline mass formed by spontaneous nucleation in the contaminated solution is visible at left. **(b)** X-ray topograph of a crystal grown from a pure seed in a solution containing 20% ovotransferrin. **(c)** Two-photon fluorescence micrograph of a HEWL crystal grown from a pure seed in a solution containing ~0.5% labeled ovotransferrin and ~4.5% unlabeled ovotransferrin. The image widths are (a) 600 μm, (b) and (c) 700 μm.

9(a), crystals grown from pure seeds in these solutions are usually well-faceted and crack-free. X-ray topographs of these crystals (e.g., Figure 9(b)) show contrast at the boundary between the seed and subsequent growth but no other evidence of disorder. Mosaic scans for seeded crystals are featureless, and mosaic FWHM values, B factors, and diffraction resolutions are indistinguishable from those of crystals grown in uncontaminated solutions. Similar seeding experiments performed using TEWL-contaminated solutions do not yield obvious improvements in crystal quality.

Figure 9(c) shows a two-photon fluorescence micrograph through the core of a crystal grown from a pure seed in a solution containing 0.5% labeled ovotransferrin and 4.5% unlabeled ovotransferrin. Crystals nucleated in such solutions usually crack and show extensive evidence of disorder in their topographs. Seeded crystals are generally perfect, even though the concentration of labeled ovotransferrin outside the seed is comparable to that in unseeded crystals.

Seeding is widely used by macromolecular crystallographers and has sometimes been used to obtain high-quality crystals from highly impure solutions. The present results provide a rationale for the use of seeding, and suggest that it should be most successful when the dominant impurities are structurally unrelated and have small bulk segregation coefficients.

### Growth Veils and Ghosts: Impurity Effects in Optical Images

Protein crystals often have visible lines ("veils" or "striations") that appear to demarcate the crystal's boundaries at different stages in its growth, as well as lines (growth "ghosts") along growth sector boundaries. Similar features widely observed in inorganic crystals are usually due to variations in impurity density produced by growth rate or temperature fluctuations that cause variations in lattice constant and refractive index.[37,43,44] Monaco and Rosenberger[17] and Thomas et al.[8] showed that these features become increasing visible in lysozyme crystals as growth solution purity is decreased. Consistent with their results, we observe pronounced optical features in HEWL crystals grown from TEWL- and ovotransferrin-contaminated solutions. Consequently, the visibility of veils and sector boundaries may be a useful diagnostic of the nonuniform impurity incorporation that can lead to crystal cracking and mosaic broadening. Such features do not, however, signify the presence of disorder that affects crystal B factors and diffraction resolutions, as indicated by the results in Table I.[‡]

### Implications for Purification Procedures

Proteins are often purified using crystallization, relying on the fact that most structurally dissimilar impurities are rejected by a growing crystal. However, commercial recrystallized lysozyme can contain significant concentrations of impurities (e.g., ovalbumin and ovotransferrin) that growth experiments indicate do not incorporate. Commercial and

[‡]Optical images are extremely sensitive to lattice constant differences. In transparent inorganic crystals, growth sector boundaries are visible when the lattice constant differs between sectors by as little as one part in $10^5$, corresponding to extremely tiny differences in impurity density.[43]

laboratory recrystallizations are induced by rapid and large changes in supersaturation that lead to rapid nucleation and the formation of a large number of small, imperfect crystals. Skouri et al.[6] noted that small crystals have a large surface-to-volume ratio, and suggested that surface adsorption of impurities could result in significant residual concentrations even if there is no bulk incorporation. But even with 100% coverage, crystals smaller than ~1 μm would be required to obtain impurity concentrations of 1%. The present results suggest another explanation: impurities may incorporate significantly in crystal cores and may decorate dislocations, other defects and sector boundaries, so that their total concentration may be large in the small, heavily defected crystals produced by rapid recrystallization. Consequently, improved separations may be realized by performing more gradual recrystallization to obtain larger crystals with larger bulk-to-core volume ratios.

## CONCLUSIONS

Macromolecular impurities are among the most important factors affecting the success of protein and virus crystal growth experiments. An understanding of the mechanisms by which they affect crystal quality will allow methods for mitigating these effects to be developed. The combination of experimental probes used here provides detailed insight into impurity effects in lysozyme. For the two distinct impurity types (and their fluorescently-labeled variants), the primary effects are a degradation of crystal mosaicity due to formation of cracks and dislocations. These imperfections arise from nonuniform impurity incorporation, which produces variations in lattice constant that create stresses driving defect formation, and from impurity effects on the perfection of the initial crystal nucleus. When, as for ovotransferrin, the nucleus is disordered and/or impurity-rich, high-quality crystals can be obtained by seeding. Neither impurity has measurable effects on crystal B factors and diffraction resolution even at relatively high incorporated densities. Although additional experiments using other proteins and impurities are needed, these results should have broad relevance in the practical growth of globular protein crystals.

## ACKNOWLEDGMENTS

We wish to thank N. Campobasso, A. Deacon, G. DeTitta, S. Ealick, C. Franck, R. Maimon, A. Malkin, P.G. Vekilov, and W. Wu for fruitful discussions, and the CHESS and MacCHESS staff for their assistance. RET acknowledges support provided by NASA (NAG8–1357 and NAG8–1574). AAC acknowledges support provided by the USRA and by NASA (NAG8–1454 and NCC8–66CC). CC and CK acknowledge support provided by a National Science Foundation Graduate Fellowship and a Department of Education Fellowship, respectively. WRZ, WWW, and the DRBIO are supported by the NIH (P412RR04224) and the NSF (BIR/CB1–9419978).

## REFERENCES

1. McPherson A. Preparation and analysis of protein crystals. Malabar: Krieger; 1982. 372 p.
2. Ducruix A, Giegé R. Crystallization of nucleic acids and proteins. Oxford: IRL; 1992. 331 p.
3. Giegé R, Lorber B, Theobald-Dietrich A. Crystallogenesis of biological macromolecules—facts and perspectives. Acta Crystallogr D 1994;50:339–350.
4. Wilson LJ, Suddath FL. Control of solvent evaporation in hen egg-white lysozyme crystallization. J Cryst Growth 1992;116:414–420.
5. Lorber B, Skouri M, Munch J-P, Giegé R. The influence of impurities on protein crystallization: the case of lysozyme. J Cryst Growth 1993;128:1203–1211.
6. Skouri M, Lorber B, Giege R, Munch J-P, Candau JS. Effect of macromolecular impurities on lysozyme solubility and crystallizability: dynamic light scattering, phase diagram, and crystal growth studies. J Cryst Growth 1995;152:209–220.
7. Ewing FL, Forsythe EL, van der Woerd M, Pusey ML. Effects of purification on the crystallization of lysozyme. J Cryst Growth 1996;160:389–397.
8. Thomas BR, Vekilov PG, Rosenberger F. Heterogeneity determination and purification of commercial hen egg-white lysozyme. Acta Crystallogr D 1996;52:776–784.
9. Abergel C, Nesa MP, Fontecilla-Camps JC. The effect of protein contaminants on the crystallization of turkey egg white lysozyme. J Cryst Growth 1991;110:11–19.
10. Forsythe E, Ewing F, Pusey ML. Studies of tetragonal lysozyme crystal-growth rates. Acta Crystallogr D 1994;50:614–619.
11. Forsythe E, Pusey ML. The effects of temperature and NaCl concentration on tetragonal lysozyme face growth-rates. J Cryst Growth 1994;139:89–94.
12. Provost K, Robert MC. Crystal growth of lysozymes in media contaminated by parent molecules: influence of gelled media. J Cryst Growth 1995;156:112–120.
13. Vekilov PG, Monaco LA, Rosenberger F. Facet morphology response to nonuniformities in nutrient and impurity supply: I. Experiments and interpretation. J Cryst Growth 1995;156:267–278.
14. Hirschler J, Fontecilla-Camps JC. Contaminant effects on protein crystal morphology in different growth environments. Acta Crystallogr D 1996;52:806–812.
15. Hirschler J, Fontecilla-Camps JC. Protein crystal growth rates are face-specifically modified by structurally related contaminants. J Cryst Growth 1997;171:559–565.
16. Vekilov PG, Rosenberger F. Dependence of lysozyme growth kinetics on step sources and impurities. J Cryst Growth 1996;158: 540–551.
17. Monaco LA, Rosenberger F. Growth and etching kinetics of tetragonal lysozyme. J Cryst Growth 1993;129:465–484.
18. Hirschler J, Halgand F, Forest E, Fontecilla-Camps JC. Contaminant inclusion into protein crystals analyzed by electrospray mass spectrometry and X-ray crystallography. Protein Sci 1998;7:185–192.
19. Malkin AJ, Kuznetsov Yu G, McPherson A. In situ atomic force microscopy studies of surface morphology, growth kinetics, defect structure and dissolution in protein crystallization. J Cryst Growth 1999;196:471–488.
20. Nakada T, Sazaki G, Miyashita S, Durbin SD, Komatsu H. Direct AFM observations of impurity effects on a lysozyme crystal. J Cryst Growth 1999;196:503–510.
21. Kurihara K, Miyashita S, Sazaki G, et al. Incorporation of impurity into a tetragonal lysozyme crystal. J Cryst Growth 1999;196:285–290.
22. Tanner BK. X-ray diffraction topography. Oxford: Pergamon; 1976. 174 p.
23. Fourme R, Ducruix A, Ries-Kautt M, Capelle B. The perfection of protein crystals probed by direct recording of Bragg reflection profiles with a quasi-planar X-ray wave. J Synch Rad 1995;2:136–142.
24. Stojanoff V, Siddons DP. X-ray topography of a lysozyme crystal. Acta Crystallogr A 1996;52:498–499.
25. Izumi K, Sawamura S, Ataka M. X-ray topography of lysozyme crystals. J Cryst Growth 1996;168:106–111.
26. Stojanoff V, Siddons DP, Monaco LA, Vekilov P, Rosenberger F. X-ray topography of tetragonal lysozyme grown by the temperature-controlled technique. Acta Crystallogr D 1997;53:588–595.
27. Dobrianov I, Finkelstein KD, Lemay SG, Thorne RE. X-ray

topographic studies of protein crystal perfection and growth. Acta Crystallogr D 1998;54:922–937.
28. Dobrianov I, Caylor C, Lemay SG, Finkelstein KD, Thorne RE. X-ray diffraction studies of protein crystal disorder. J Cryst Growth 1999;196:511–523.
29. Fourme R, Ducruix A, Ries-Kautt M, Capelle B. Probing the quality of macromolecular crystals using bragg reflection profiles, X-ray topographs and resolution of diffraction data. J Cryst Growth 1999;196:535–545.
30. Vidal O, Robert M-C, Capelle B, Arnoux B. Study of crystalline quality by X-ray diffraction techniques of lysozyme crystals grown in agarose and silica gels. J Cryst Growth 1999;196:559–571.
31. Otalora F, Garcia-Ruiz J-M, Gavira J-A, Capelle B. Topography and high-resolution diffraction studies in tetragonal lysozyme. J Cryst Growth 1999;196:546–558.
32. Shaikevitch A, Kam Z. Investigation of long-range order in protein crystals by X-ray diffraction. Acta Crystallogr A 1981;37:871–875.
33. Helliwell JR. Protein crystal perfection and the nature of radiation-damage. J Cryst Growth 1988;90:259–272.
34. Snell EH, Weisgerber S, Helliwell JR, Weckert E, Holzer K, Schroer K. Improvements in lysozyme protein crystal perfection through microgravity growth. Acta Crystallogr D 1995;51:1099–1102.
35. Denk W, Strickler JH, Webb WW. 2-photon laser scanning fluorescence microscopy. Science 1990;248:73–76.
36. Xu C, Zipfel W, Ster JB, Williams RM, Webb WW. Multiphoton fluorescence excitation: new spectral windows for biological nonlinear microscopy. Proc Nat Acad Sci USA 1996;93:10763–10768.
37. Chernov AA. Modern crystallography III. Crystal growth. Berlin: Springer; 1984. 517 p.
38. Chernov AA. Crystals built of biological macromolecules. Physics Reports 1997;288:61–75.
39. Vekilov PG, Monaco LA, Thomas BR, Stojanoff V, Rosenberger F. Repartitioning of NaCl and protein impurities in lysozyme crystallization. Acta Crystallogr D 1996;52:785–798.
40. Chernov AA, Komatsu H. In: van der Eerden JP, Bruinsma OSL, editors. Principles of crystal growth in protein crystallization. Science and technology of crystal growth. Dordrecht: Kluwer; 1995. p 329–353.
41. Krivoglaz MA. X-ray and neutron diffraction in nonideal crystals. Berlin: Springer; 1996. 174 p.
42. Shternberg AA. Heterometry: the relation of morphology to cracking in crystals containing impurities. Soviet Phys-Cryst 1962;7:92–96.
43. Treivus EB, Petrov TG, Kamentsev IE. Formation of dislocations at the boundaries of crystal growth pyramids. Soviet Phys-Cryst 1965;10:305–308.
44. Belouet C, Monnier M, Verplanke JC. Autoradiography as a tool for studying iron segregation and related defects in $KH_2PO_4$ single crystals. J Cryst Growth 1975;29:109–120.
45. Durbin SD, Feher G. Crystal growth studies of lysozyme as a model for protein crystallization. J Cryst Growth 1986;76:583–592.
46. Vekilov PG. Nonlinear dynamics of layer spreading and consequences for protein crystal growth and quality. J Cryst Growth 1999;196:261–275.
47. Koz'ma AA, Arinkin AV, Mikhay'lov IF, Fuks M. Ya. Fiz. Metal. Metalloved 1973;36:596–604. (English transl.: Investigation of structural imperfections in deformed metals by X-ray diffraction. Phys Metals Metallogr 1973;38:132–140.).